

## Experimental paper

## Dose optimization of early high-dose valproic acid for neuroprotection in a swine cardiac arrest model



Cindy H. Hsu<sup>a,b,c,\*</sup>, Mohamad H. Tiba<sup>a,b</sup>, Brendan M. McCracken<sup>a,b</sup>, Carmen I. Colmenero<sup>a,b</sup>, Zachary Pickell<sup>a,d</sup>, Danielle C. Leander<sup>a,b</sup>, Anne M. Weitzel<sup>a,b</sup>, Sarita Raghunayakula<sup>a</sup>, Jinhui Liao<sup>a</sup>, Tulasi Jinka<sup>a,b</sup>, Brandon C. Cummings<sup>a,b</sup>, Manjunath P. Pai<sup>e</sup>, Hasan B. Alam<sup>b,c</sup>, Kevin R. Ward<sup>a,b,f</sup>, Thomas H. Sanderson<sup>a,b,g</sup>, Robert W. Neumar<sup>a,b</sup>

<sup>a</sup> Department of Emergency Medicine, University of Michigan Medical School, Ann Arbor, MI, USA

<sup>b</sup> Michigan Center for Integrative Research in Critical Care, University of Michigan Medical School, Ann Arbor, MI, USA

<sup>c</sup> Department of Surgery, University of Michigan Medical School, Ann Arbor, MI, USA

<sup>d</sup> College of Literature Science and the Arts, University of Michigan Medical School, Ann Arbor, MI, USA

<sup>e</sup> Department of Clinical Pharmacy, College of Pharmacy, University of Michigan Medical School, Ann Arbor, MI, USA

<sup>f</sup> Department of Biomedical Engineering, University of Michigan Medical School, Ann Arbor, MI, USA

<sup>g</sup> Department of Molecular and Integrative Physiology, University of Michigan Medical School, Ann Arbor, MI, USA

## ARTICLE INFO

## Keywords:

Cardiac arrest

Swine model

Valproic acid

Histone acetylation

Pharmacokinetic

Pharmacodynamics biomarker

## ABSTRACT

**Aim:** High-dose valproic acid (VPA) improves the survival and neurologic outcomes after asphyxial cardiac arrest (CA) in rats. We characterized the pharmacokinetics, pharmacodynamics, and safety of high-dose VPA in a swine CA model to advance clinical translation.

**Methods:** After 8 min of untreated ventricular fibrillation CA, 20 male Yorkshire swine were resuscitated until return of spontaneous circulation (ROSC). They were block randomized to receive placebo, 75 mg/kg, 150 mg/kg, or 300 mg/kg VPA as 90-min intravenous infusion (n = 5/group) beginning at ROSC. Animals were monitored for 2 additional hours then euthanized. Experimental operators were blinded to treatments.

**Results:** The mean(SD) total CA duration was 14.8(1.2) minutes. 300 mg/kg VPA animals required more adrenaline to maintain mean arterial pressure  $\geq 80$  mmHg and had worse lactic acidosis. There was a strong linear correlation between plasma free VPA  $C_{max}$  and brain total VPA ( $r^2 = 0.9494$ ;  $p < 0.0001$ ). VPA induced dose-dependent increases in pan- and site-specific histone H3 and H4 acetylation in the brain. Plasma free VPA  $C_{max}$  is a better predictor than peripheral blood mononuclear cell histone acetylation for brain H3 and H4 acetylation ( $r^2 = 0.7189$  for H3K27ac,  $r^2 = 0.7189$  for pan-H3ac, and  $r^2 = 0.7554$  for pan-H4ac;  $p < 0.0001$ ).

**Conclusions:** Up to 150 mg/kg VPA can be safely tolerated as 90-min intravenous infusion in a swine CA model. High-dose VPA induced dose-dependent increases in brain histone H3 and H4 acetylation, which can be predicted by plasma free VPA  $C_{max}$  as the pharmacodynamics biomarker for VPA target engagement after CA.

## Introduction

Sudden cardiac arrest (CA) is a leading cause of death in the U.S., affecting approximately 430,000 individuals annually with an overall mortality rate of close to 90%.<sup>1</sup> Furthermore, approximately two-third of

the patients resuscitated from out-of-hospital CA ultimately die from neurologic injury,<sup>2</sup> and up to half of the survivors have cognitive dysfunction.<sup>3-5</sup> No pharmacologic agent has yet been established as neuroprotective for CA victims.

VPA is an antiepileptic medication with neuroprotective properties in

\* Corresponding author. Department of Emergency Medicine, Department of Surgery, Michigan Center for Integrative Research in Critical Care, University of Michigan Medical School, NCRB B026-309N, 2800 Plymouth Road, Ann Arbor, MI, 48109-2800, USA.

E-mail addresses: [hcindy@med.umich.edu](mailto:hcindy@med.umich.edu) (C.H. Hsu), [tibam@med.umich.edu](mailto:tibam@med.umich.edu) (M.H. Tiba), [bmccrac@med.umich.edu](mailto:bmccrac@med.umich.edu) (B.M. McCracken), [cico@med.umich.edu](mailto:cico@med.umich.edu) (C.I. Colmenero), [zpickell@umich.edu](mailto:zpickell@umich.edu) (Z. Pickell), [danlean@umich.edu](mailto:danlean@umich.edu) (D.C. Leander), [weitzela@umich.edu](mailto:weitzela@umich.edu) (A.M. Weitzel), [raghunay@med.umich.edu](mailto:raghunay@med.umich.edu) (S. Raghunayakula), [jinhuil@med.umich.edu](mailto:jinhuil@med.umich.edu) (J. Liao), [tjinka@med.umich.edu](mailto:tjinka@med.umich.edu) (T. Jinka), [cummingsb@med.umich.edu](mailto:cummingsb@med.umich.edu) (B.C. Cummings), [amitpai@med.umich.edu](mailto:amitpai@med.umich.edu) (M.P. Pai), [alamh@med.umich.edu](mailto:alamh@med.umich.edu) (H.B. Alam), [keward@med.umich.edu](mailto:keward@med.umich.edu) (K.R. Ward), [thsand@med.umich.edu](mailto:thsand@med.umich.edu) (T.H. Sanderson), [neumar@med.umich.edu](mailto:neumar@med.umich.edu) (R.W. Neumar).

<https://doi.org/10.1016/j.resplu.2020.100007>

Received 23 March 2020; Received in revised form 1 May 2020; Accepted 11 May 2020

2666-5204/© 2020 The Author(s). Published by Elsevier B.V. This is an open access article under the CC BY-NC-ND license (<http://creativecommons.org/licenses/by-nc-nd/4.0/>).

various preclinical models of brain injury.<sup>6–8</sup> Its proposed neuroprotective mechanisms are pleiotropic, including histone deacetylase inhibition,<sup>9,10</sup> survival kinase activation,<sup>8,11–14</sup> and antiepileptic properties.<sup>15</sup> Two independent laboratories have demonstrated that early high-dose VPA (300 mg/kg) improves survival and neurologic outcomes when given alone or in combination with hypothermic targeted temperature management after asphyxial CA in rats.<sup>16–18</sup> Furthermore, 150 mg/kg VPA significantly decreases the neurologic injury and expedites functional recovery in a swine model of combined traumatic brain injury and haemorrhagic shock.<sup>19,20</sup> A recent phase 1a clinical study showed that up to 140 mg/kg intravenous VPA (a dose much higher than the Food and Drug Administration approved 15–60 mg/kg/day) can be safely tolerated by healthy volunteers.<sup>21</sup>

To translate high-dose VPA to early phase clinical trials, it would be advantageous to first determine its safety in a large animal model of CA. Furthermore, it is important to identify peripheral pharmacodynamics biomarkers that can accurately validate VPA's mechanistic target engagement and efficacious dose. Therefore, we sought out to elucidate the pharmacokinetic, pharmacodynamics, and safety of early high-dose VPA in a clinically relevant swine CA model.

## Methods

All procedures outlined in this study adhered to the 8th edition of the Guide for the Care and Use of Laboratory Animals<sup>22</sup> and were approved by the University of Michigan Institutional Animal Care and Use Committee.

### Animal model

Anesthetized adolescent male Yorkshire swine (40–50 kg; Michigan State University, East Lansing, MI) were intubated, placed on a mechanical ventilator, and instrumented for haemodynamic monitoring. To simulate witnessed out-of-hospital CA without bystander cardiopulmonary resuscitation (CPR), the animals were subjected to 8 min of untreated ventricular fibrillation CA induced with a pacing wire into the right ventricle using a 9-V battery, followed by CPR and advanced life support for up to 16 additional minutes until return of spontaneous circulation (ROSC). We defined ROSC as an organized cardiac rhythm with systolic blood pressure above 80 mmHg for more than 20 min with or without vasopressor infusion. The animals were block randomized to receive placebo (normal saline), 75 mg/kg, 150 mg/kg, or 300 mg/kg VPA in 300 mL normal saline as a 90-min intravenous infusion beginning at ROSC (n = 5/group). The animals were monitored for 2 additional hours after end of infusion and then euthanized with 2 mEq/kg intravenous potassium chloride. Experimental operators were blinded to the treatments. Sham-operated control animals (n = 4) were also included (Supplemental Figure 1). To limit variability in secondary neurologic injury, we standardized post-CA care by maintaining all animals at normothermia (37–38 °C) on a warming blanket (Blanketrol1, Cincinnati Sub-Zero, Cincinnati, OH), normoxia (SpO<sub>2</sub> 94–98% or PaO<sub>2</sub> 100–200 mmHg), eucapnia (PaCO<sub>2</sub> 35–45 mmHg), euglycemia (glucose 60–180 mg/dL), and mean arterial pressure (MAP) above 80 mmHg with adrenaline (epinephrine) infusion. Continuous waveform haemodynamic data were collected using Biopac Data Acquisition System (Biopac Systems Inc. Goleta, CA). Detailed experimental protocol is described in Supplemental Figure 2.

### Experimental outcomes

The primary outcome was VPA pharmacokinetics of at least 2-fold change in VPA maximum concentration (C<sub>max</sub>) between groups. The secondary outcomes were haemodynamic safety as measured by adrenaline requirement to maintain MAP above 80 mmHg and VPA pharmacodynamics as measured by histone H3 and H4 acetylation in the brain.

### Sample size calculation

We based our power calculation on historical data<sup>17,23</sup> and pilot studies from our laboratories. In order to achieve  $\alpha = 0.05$  and 80% power to detect at least 2 fold-change in VPA C<sub>max</sub> between groups, a minimum of 5 surviving animals per group was needed.

### Sample preparations

Blood samples were collected at baseline prior to CA, at end of treatment infusion, and at 1 h and 2 h post-infusion. Peripheral blood mononuclear cells (PBMC) were isolated using Ficoll-Paque™ density gradient as previously described.<sup>24</sup> The animals were euthanized 2 h post-infusion, and their brains were removed and dissected on ice. All brain samples were then immediately flash frozen and stored at -80 °C for future analysis.

### Pharmacokinetic analysis

Details of the pharmacokinetic sample preparation, assays, and analysis have been previously described.<sup>23</sup> The VPA concentration time data were described descriptively and also co-modelled through population pharmacokinetic analysis using the non-parametric adaptive grid algorithm in the Pmetrics™ library evoked through R.<sup>25</sup> Multiple models were tested to incorporate saturable protein binding with discrimination using the Akaike information criteria, non-parametric distributional error, and goodness-of-fit measures. The final model was used to generate predicted plasma and brain concentration-time profiles of VPA based on the tested doses and 1000 subject/dose level Monte Carlo Simulations for non-compartmental exposure estimates.

### Western blot

Hippocampal and PBMC samples were homogenized in RIPA buffer on ice. 15 to 30 mcg protein lysate per lane were resolved under denaturing condition on 4–20% gradient Mini-PROTEAN® TGX™ precast gels (Bio-Rad, Hercules, CA), then transferred onto nitrocellulose membrane. After blocking at room temperature for 1 h in Tris-buffered saline-0.1% Tween 20 (TBST) containing 5% nonfat dry milk or bovine serum albumin, the transferred membranes were incubated with primary antibodies (Supplemental Figure 3) at 4 °C overnight. After washing in TBST, the membranes were incubated with the appropriate secondary antibody-HRP conjugates. The protein bands were visualized using Pierce ECL substrate (ThermoFisher, Waltham, MA), and images were captured with ChemDoc™ XRS+ system (Bio-Rad, Hercules, CA). Acetylated histone signals were expressed relative to their corresponding total histone levels, while phosphoprotein signals were expressed relative to their corresponding total protein levels. Thereafter, the fold-change was expressed relative to the sham group.  $\beta$ -actin levels were used to normalize protein loading. Quantifications were performed with Image J (NIH, Bethesda, MD).

### Statistical analysis

Data were presented as mean and standard deviation (SD). One-way analysis of variance (ANOVA) with post-hoc Tukey's correction for multiple comparisons was used to compare continuous variables. Bartlett's and Brown-Forsythe tests were used to assess SD equality. Categorical variables were compared with chi-squared test. Linear regression was used to determine correlations between continuous variables. A p value < 0.05 was considered statistically significant. Prism 8 (GraphPad, LaJolla, CA) and MATLAB R2017b (The Mathworks, Inc., Natick, MA) were used for data analysis.

## Results

### Animal characteristics

All 24 animals including 20 swine that underwent CA/randomization and 4 sham-operated controls survived until the end of experiment. The mean total CA duration was 14.8(1.2) minutes, with no significant differences between experimental groups. There were no significant inter-group differences in weight, pre-CA temperature, baseline haemodynamic, baseline arterial blood gas, and total lactated Ringer's solution received from ROSC to 2 h post-infusion. There were also no differences between the number of animals that had received lidocaine during CA or dextrose and sodium bicarbonate after ROSC (Table 1). Finally, there were no differences in white blood cell counts, haemoglobin, platelets, or hepatic enzymes between baseline and 2 h post-infusion of each animal and between groups (data not shown).

**Table 1**  
Animal characteristics.

Characteristic	Mean (SD)				p value
	Placebo	75 mg/kg VPA	150 mg/kg VPA	300 mg/kg VPA	
Weight (kg)	42 (3)	44 (2)	45 (3)	42 (3)	0.134
Pre-cardiac arrest temperature (°C)	37.6 (0.5)	37.5 (0.4)	37.9 (0.5)	37.3 (0.6)	0.532
<b>Baseline haemodynamics</b>					
MAP (mmHg)	96 (19)	80 (10)	90 (11)	76 (11)	0.110
DBP (mmHg)	70 (11)	70 (11)	80 (9)	67 (12)	0.314
CPP (mmHg)	61 (12)	62 (13)	70 (9)	59 (10)	0.432
Heart rate (bpm)	92 (10)	87 (14)	91 (16)	89 (11)	0.916
<b>Baseline arterial blood gas</b>					
pH	7.46 (0.02)	7.49 (0.07)	7.46 (0.05)	7.44 (0.12)	0.727
PaCO <sub>2</sub> (mmHg)	39 (3)	35 (5)	38 (5)	39 (4)	0.543
PaO <sub>2</sub> (mmHg)	129 (26)	133 (7)	128 (15)	136 (32)	0.917
HCO <sub>3</sub> (mmol/L)	29 (2)	29 (2)	28 (1)	27 (5)	0.577
Lactate (mmol/L)	1.3 (0.5)	1.5 (1.2)	1.1 (0.4)	1.9 (0.9)	0.474
Glucose (mg/dL)	112 (57)	89 (9)	81 (23)	84 (14)	0.435
Duration of cardiac arrest (minutes)	14.8 (1.1)	15.2 (1.8)	14.8 (1.1)	14.4 (0.9)	0.801
<b>Fluid &amp; Medications</b>					
Lactated Ringer's solution, ROSC to 2hr post-infusion (mL)	520 (500)	550 (570)	490 (410)	665 (505)	0.949
Lidocaine (number of animals)	2/5	3/5	3/5	2/5	0.850
Dextrose after ROSC (number of animals)	0/5	1/5	1/5	0/5	0.528
Sodium bicarbonate after ROSC (number of animals)	0/5	1/5	0/5	1/5	0.528
<b>Epinephrine</b>					
Prior to treatment infusion (mcg)	2266 (674)	2028 (756)	2120 (877)	1864 (646)	0.855
Prior to treatment infusion (mcg/kg/min)	3.21 (1.74)	3.57 (1.08)	2.72 (0.80)	2.32 (0.52)	0.348
Start of treatment infusion to 2hr post-infusion (mcg)	2036 (518)	1851 (648)	1865 (714)	3752 (1684)	p < 0.05 <sup>&amp;</sup>
Start of treatment infusion to 2hr post-infusion (mcg/kg/min)	0.23 (0.07)	0.20 (0.07)	0.19 (0.06)	0.43 (0.21)	p < 0.05 <sup>&amp;</sup>

SD = standard deviation; VPA = valproic acid; MAP = mean arterial pressure; DBP = diastolic blood pressure; CPP = coronary perfusion pressure; bpm = beats per minute; ROSC = return of spontaneous circulation; <sup>&</sup>300 mg/kg vs 75 mg/kg VPA; <sup>§</sup>300 mg/kg vs 150 mg/kg VPA; One-way ANOVA with post-hoc Tukey's.

### Haemodynamic

There was no significant difference in the temperature, haemodynamic parameters, PaCO<sub>2</sub>, and PaO<sub>2</sub> from start of treatment infusion until 2 h post-infusion between groups. Serum glucose levels were maintained above 60 mg/dL for all groups (Fig. 1A and Supplemental Figure 4). The 300 mg/kg VPA group required significantly more adrenaline to maintain MAP ≥ 80 mmHg during treatment infusion than the 75 mg/kg and 150 mg/kg VPA groups (p < 0.05; Table 1 and Fig. 1B). It also had significantly worse lactic acidosis than the placebo and 75 mg/kg groups (p < 0.005; Fig. 1C and Supplemental Figure 4).

### High-dose VPA pharmacokinetics after CA

At end of VPA infusion, the mean plasma free VPA C<sub>max</sub> increased dose dependently from 139(10) mcg/mL to 287(25) mcg/mL to 566(37) mcg/mL for 75, 150, and 300 mg/kg VPA, respectively (p < 0.05; Supplemental Figure 5). The dose-dependent increase in mean plasma total VPA C<sub>max</sub> were 239(19) mcg/mL to 376(35) mcg/mL to 662(43) mcg/mL for 75, 150, and 300 mg/kg VPA, respectively (p < 0.05; Supplemental Figure 5). These increases corresponded to a dose-dependent decrease in the fraction of serum protein-bound VPA, from 41.8%(1.8) to 23.4%(3.8) to 14.4%(3.8) for 75, 150, and 300 mg/kg VPA at end infusion, respectively (p < 0.0001). Mean brain total VPA concentrations at 2 h post-infusion were 26(3) mcg/g for 75 mg/kg VPA, 73(19) mcg/g for 150 mg/kg VPA, and 212(33) mcg/g for 300 mg/kg VPA (p < 0.05; Supplemental Figure 5). Pharmacokinetic modelling revealed that a 3-compartment model adequately characterized the plasma total and free VPA concentrations as well as the brain concentrations. This model incorporated the saturable plasma protein binding of VPA. Monte Carlo Simulations generated estimated C<sub>max</sub> values that matched observed values and projection of the area under the curve from time 0 to infinity (AUC<sub>inf</sub>) for comparison with clinical data. The projected time to maximum brain concentration and terminal half-life is a median [IQR] of 8.5 [7, 10.5] hours and 14.5 [9.9, 21] hours, respectively. The model structure, parameter estimates, and projected total VPA C<sub>max</sub>, AUC<sub>inf</sub>, and half-life with the tested doses are provided to aid human dose translation (Supplemental Figure 6).

Taken together, our data showed that VPA crosses the blood-brain-barrier dose-dependently in a linear fashion after CA in swine (r<sup>2</sup> = 0.9327, p < 0.0001; Fig. 2A). There was also a strong linear correlation between plasma free VPA C<sub>max</sub> and brain total VPA concentrations (r<sup>2</sup> = 0.9494, p < 0.0001; Fig. 2B).

### Plasma free VPA C<sub>max</sub> predicts the dose-dependent increase of hippocampal histone H3 and H4 acetylation induced by VPA

We examined the VPA-induced changes in hippocampal histone H3 and H4 acetylation using western blot analysis. We observed 2 to 3-fold dose-dependent increase in hippocampal pan-acetylated histone H3 (pan-H3ac). More specifically, we observed a 3-fold increase in acetylated H3K9 (H3K9ac) in the 300 mg/kg VPA group and 2 to 8-fold dose-dependent increase in acetylated H3K27 (H3K27ac; Fig. 3A). We also observed 3 to 9-fold dose-dependent increases in pan-acetylated histone H4 (pan-H4ac) and H4K8 (H4K8ac) (Fig. 3B). Furthermore, we found that plasma free VPA C<sub>max</sub> predicts the levels of hippocampal H3K27ac (r<sup>2</sup> = 0.7189, p < 0.001; Fig. 3C), pan-H3ac (r<sup>2</sup> = 0.7189, p < 0.0001; Fig. 3D), and pan-H4ac (r<sup>2</sup> = 0.7554, p < 0.001; Fig. 3E). However, there were no significant differences in Akt and mTOR phosphorylation or β-catenin and α-tubulin acetylation between the groups (Supplemental Figure 7).

### PBMC pan-acetylated histone H3 and H4 correlate weakly with their respective changes in the brain

We determined whether PBMC histone H3 and H4 acetylation reflect changes observed in the brain and could serve as reliable peripheral pharmacodynamics biomarkers. Western blots of PBMC collected at 2 h

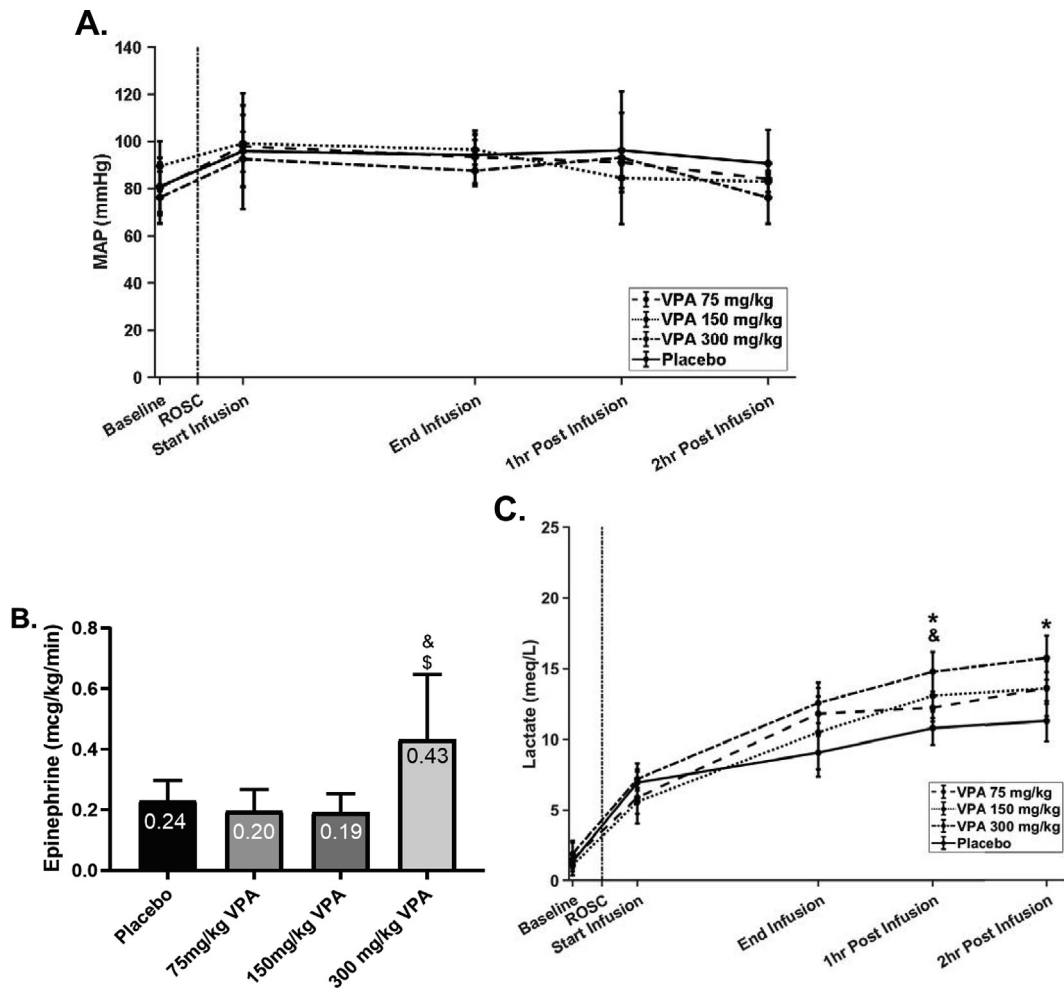


**Fig. 1.** Haemodynamic, adrenaline requirement, and lactic acidosis comparisons between treatment groups. A) Mean arterial pressure (MAP)  $\geq 80$  mmHg were maintained with adrenaline infusion and fluid for all groups. However, 300 mg/kg VPA swine required significantly B) more adrenaline to maintain MAP  $\geq 80$  mmHg than 75 mg/kg (&) and 150 mg/kg VPA (\$) groups ( $p < 0.05$ ). It also had C) significantly higher lactic acidosis than placebo (\*) and 75 mg/kg (&) groups at 1 h post-infusion ( $p < 0.005$ ) and higher than placebo (\*) at 2 h post-infusion ( $p < 0.005$ ). One-way ANOVA with post-hoc Tukey's was performed for all comparisons. VPA = valproic acid.

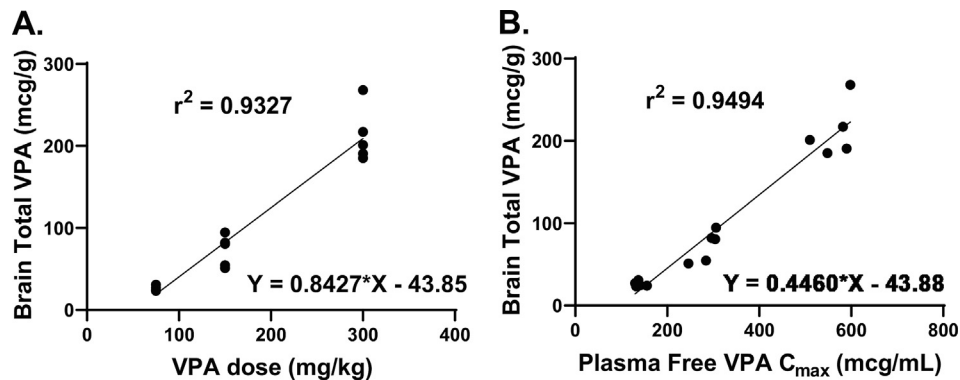


**Fig. 2.** Valproic acid pharmacokinetic analysis after cardiac arrest. A) VPA crosses the blood-brain-barrier dose dependently in a linear fashion after CA in swine ( $r^2 = 0.9327$ ,  $p < 0.0001$ ). B) Plasma free VPA  $C_{max}$  correlated linearly with brain total VPA after CA in swine ( $r^2 = 0.9494$ ,  $p < 0.0001$ ). VPA  $C_{max}$  = VPA maximum concentration measured at end infusion. Brain total VPA levels were measured at 2 h post-infusion. VPA = valproic acid.

post-infusion demonstrated 2-fold dose-dependent increase in pan-H3ac, but not in H3K9ac or H3K27ac levels (Fig. 4A). Similarly, there was a 2-fold increase in PBMC pan-H4ac but not H4K8ac for the 300 mg/kg VPA

group (Fig. 4B). We observed weak positive correlations between PBMC pan-H3ac ( $r^2 = 0.307$ ,  $p < 0.05$ ; Fig. 4C) and pan-H4ac levels ( $r^2 = 0.307$ ,  $p < 0.05$ ; Fig. 4D) with their respective changes in the hippocampus.

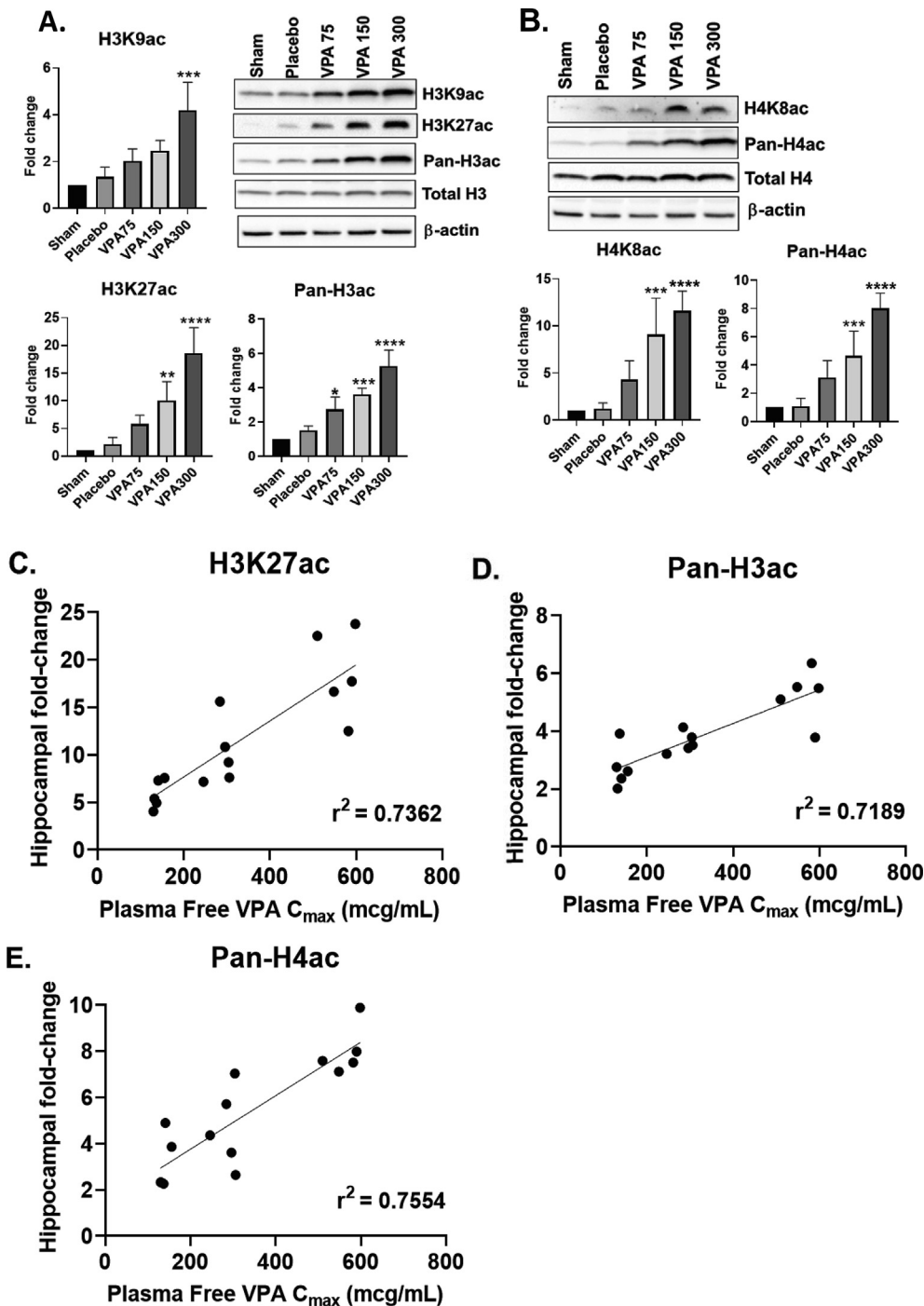


**Fig. 3.** Early high-dose valproic acid induces dose-dependent increases in hippocampal histone H3 and H4 acetylation at 2 h after infusion. **A)** Early high-dose VPA increases hippocampal H3K9ac, H3K27ac, and pan-H3ac levels dose-dependently at 2 h post-infusion. It also increases **B)** hippocampal H4K8ac and pan-acetylated histone H4 levels dose-dependently at 2 h post-infusion. Plasma free VPA  $C_{max}$  predicts **C)** H3K27ac ( $r^2 = 0.7362$ ,  $p < 0.0001$ ), **D)** pan-acetylated H3 ( $r^2 = 0.7189$ ,  $p < 0.0001$ ), and **E)** pan-acetylated H4 levels in the brain ( $r^2 = 0.7554$ ,  $p < 0.001$ ). One-way ANOVA with post-hoc Tukey's: \* $p < 0.05$ ; \*\* $0.01$ ; \*\*\* $0.001$ ; \*\*\*\* $0.0001$  compared to placebo. H3 = histone H3; H4 = histone H4; VPA = valproic acid; ac = acetylated.

## Discussion

We have demonstrated that swine could tolerate up to 150 mg/kg VPA as a 90-min intravenous infusion after CA without the need for additional vasopressors. While we were able to maintain all animals at  $MAP \geq 80$  mmHg with adrenaline infusion (Fig. 2A), the 300 mg/kg VPA group did require significantly higher amount of adrenaline (Fig. 2B) and had worse lactic acidosis (Fig. 2C). The cause of haemodynamic effects and lactic acidosis for the 300 mg/kg VPA group was likely multifactorial, including drug infusion rate and increased adrenaline requirement.<sup>13,19,23,26</sup> Our pharmacokinetic analysis showed that VPA crossed the blood-brain-barrier in a linear, dose-dependent fashion, and that plasma free VPA  $C_{max}$  correlated strongly with brain total VPA level.

These findings suggest that we could use the plasma free VPA  $C_{max}$  to predict the amount of drug penetration in the brain. Furthermore, we found that VPA induced dose-dependent increases in pan- and site-specific histone H3 (H3K9ac, H3K27ac) and H4 (H4K8ac) acetylation in the brain. Finally, we found that plasma free VPA  $C_{max}$  predicts histone H3K27, pan-H3, and pan-H4 acetylation in the brain better than PBMC histone acetylation, which suggest that plasma free VPA  $C_{max}$  can be used as a peripheral pharmacodynamics biomarker for VPA target engagement after CA. These results provide the foundation for early phase dose-optimization clinical studies of high-dose VPA as a neuro-protective therapy following resuscitation from CA.

Our findings support starting with 150 mg/kg VPA for our subsequent swine CA neurocognitive studies. The robust 2–7 fold increases in

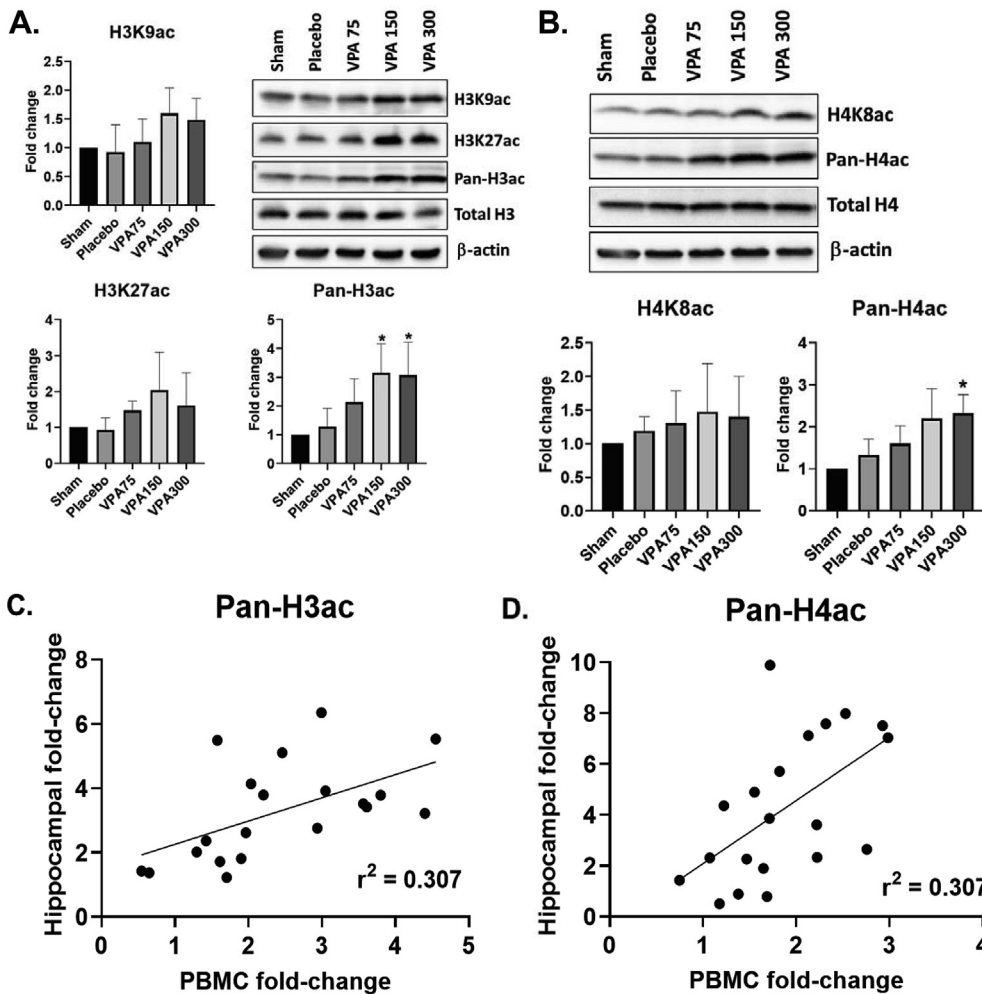


**Fig. 4.** Early high-dose valproic acid induces dose-dependent increases in peripheral blood mononuclear cell pan-acetylated histone H3 and H4 levels at 2 h after infusion. Early high-dose VPA induces dose dependent increases in PBMC **A)** pan-acetylated H3 ( $r = 0.5536$ , 95% CI 0.1471–0.8001,  $p < 0.05$ ) and **B)** pan-acetylated H4 levels at 2 h post-infusion. One-way ANOVA with post-hoc Tukey's:  $*p < 0.05$  compared to placebo. The fold-change relative to sham in PBMC **C)** pan-acetylated H3 ( $r = 0.5536$ , 95% CI 0.1471–0.8001,  $p < 0.05$ ) and **D)** pan-acetylated H4 levels ( $r = 0.5542$ , 95% CI 0.1479–0.8004,  $p < 0.05$ ) correlated with their respective fold-change in the hippocampus. PBMC = peripheral blood mononuclear cells. H3 = histone H3; H4 = histone H4; VPA = valproic acid; ac = acetylated.

acetylated histone H3 and H4 compared to placebo with this dose should be sufficient to induce detectable transcriptomic changes in the brain. Previous studies have demonstrated that a dose of 150 mg/kg VPA decreased neurologic injury and expedited neurologic recovery in a swine polytrauma model.<sup>23</sup> A dose-optimization study showed that 150 mg/kg VPA significantly improved survival in a swine model of lethal polytrauma when administered over 3 h at 1 h after shock. This protection was lost when the VPA dose was lowered to 100 mg/kg over 3 h but restored when the same dose was infused over 2 h.<sup>20</sup> These findings suggest that while the dose of VPA may be critical for its protective effect, its infusion rate and associated  $C_{max}$  may be equally important. We demonstrated that 150 mg/kg as a 90-min infusion achieved mean plasma total VPA  $C_{max}$  of 376 mcg/mL and free VPA  $C_{max}$  of 287 mcg/mL. These levels were much higher than the levels observed in prior protective swine studies. Biesterveld et al found that protective doses of 150 mg/kg VPA as a 3-h infusion achieved a total VPA  $C_{max}$  of 175 mcg/mL while 100 mg/kg VPA as a 2-h infusion achieved a total  $C_{max}$  of 115 mcg/mL.<sup>20</sup> Similarly, Nikolian et al found that 150 mg/kg VPA given as a 3-h infusion achieved a 145 mcg/mL mean total VPA  $C_{max}$  level, and that this dose reduced neurologic injury and expedited recovery after polytrauma.<sup>23</sup> The differences in the plasma VPA levels between the CA and trauma models may be due to differences in intravascular volume, temperature, volume of distribution, and drug elimination. The observed VPA  $C_{max}$  levels and model predicted  $AUC_{inf}$  achieved in our study correlated to 60–90 mg/kg administered as 1-h infusion in healthy human subjects based on cross-species and phase 1a trial pharmacokinetics studies.<sup>17,20,21,23</sup>

Although VPA induced robust increases in brain histone H3 and H4 acetylation after CA, we did not observe significant changes in downstream pro-survival signalling pathways including Akt, mTOR,  $\beta$ -catenin,

and  $\alpha$ -tubulin. This could be explained by our early, single time-point experimental design. We chose to focus on 2 h post-infusion based on the robust dose-dependent increases in acetylated histone H3 and H4. H3K9ac is indicative of active gene expression in the euchromatin state, while H3K27ac is indicative of an active enhancer-promoter state.<sup>27</sup> VPA, through the hyperacetylation of histone H3K9, leads to chromatin decondensation.<sup>28–30</sup> The concomitant demethylations at this same site disrupt the structural integrity of lamina-associated domains and transcriptional repression located on the inner surface of the nuclear membrane,<sup>31–33</sup> leading to the induction of neurogenesis<sup>34–37</sup> and neuronal de-differentiation.<sup>38</sup> Prior studies have demonstrated conflicting results in pro-survival signalling pathways induced by high-dose VPA. Oh et al did not observe any differences in rat asphyxial CA model in Akt, ERK1/2, or HSP70 at 24 h after ROSC.<sup>17</sup> However, high-dose VPA has been associated with upregulations of HSP70,<sup>11</sup> HIF-1 $\alpha$ ,<sup>12</sup> Akt,<sup>8,13</sup> GSK-3 $\beta$ ,<sup>8,13</sup> bcl-2,<sup>13</sup>  $\beta$ -catenin,<sup>13</sup> ERK,<sup>8</sup> JNK,<sup>14</sup> and NF- $\kappa$ B<sup>14</sup> in brain or liver at different time points in trauma or hypothermia models. High-throughput RNA sequencing studies are currently underway to determine the transcriptomic effects of high-dose VPA after CA.

Our study is the first to examine the correlations between proteomic changes in the brain with peripheral cells using a large animal CA model. Our findings of more robust correlations between plasma free VPA  $C_{max}$  and brain histone acetylation than PBMC with the brain are consistent with results from clinical studies of high-dose VPA for solid tumour malignancies.<sup>39</sup> Similar to these studies, we also observed notable inter-subject variabilities in PBMC acetylated H3 and H4 levels in addition to less robust overall increase compared to the brain. Munster et al found that all solid tumour patients who responded to VPA treatment had

more than 2-fold increase in their PBMC acetylated H4 levels with significant inter-patient variabilities.<sup>40</sup> Taken together, data from our studies and others suggest that VPA-induced proteomic changes may lead to variable effects dependent on disease state, tissue type, and patient phenotype. Further studies are necessary to determine whether individual variabilities in plasma free VPA  $C_{max}$  and PBMC histone H3 and H4 acetylation correlate to differences in response to VPA after CA.

This study has several limitations. Only male swine were used in order to achieve an adequate sample size for the pharmacokinetic and safety analyses. To address this limitation, we are performing a VPA dose-optimization study powered to detect differences in neurocognitive outcomes that includes swine from both sexes. Another limitation is that we only examined histone acetylation at a single time-point in order to correlate their levels in the PBMC with that of the brain. It is possible that other histone acetylation or methylation sites may be more predictive pharmacodynamics biomarkers. Given that the overall magnitude of change in PBMC was much less than in the brain, this study might be underpowered to detect differences in other pharmacodynamics biomarkers in PBMCs. Finally, the survival and neuroprotective benefits, therapeutic window, and minimal dose required to achieve maximal protection for high-dose VPA after CA still need to be validated in the swine model before translation to early phase clinical studies.

## Conclusions

High-dose VPA can be safely tolerated up to 150 mg/kg as a 90-min intravenous infusion after CA in a swine model. It crosses the blood-brain-barrier in a linear fashion, and plasma free VPA  $C_{max}$  can be used to predict VPA brain penetration. High-dose VPA induced dose-dependent increases in pan- and site-specific histone H3 and H4 acetylation in the brain. Plasma free VPA  $C_{max}$  predicts histone H3 and H4 acetylation in the brain, thus can be used as a pharmacodynamics biomarker for VPA target engagement after CA.

## Acknowledgments

This work was presented at the 2019 Resuscitation Science Symposium poster session in Philadelphia, PA, on November 17, 2019. Dr. Hsu reports research grant K12HL133304-01 from the National Institutes of Health. Dr. Neumar reports research grants NIH-R01HL133129, NIH-R44HL091606, and NIH-R34HL130738 from the National Institutes of Health and equipment support for clinical and laboratory research from Physio-Control.

## Appendix A. Supplementary data

Supplementary data to this article can be found online at <https://doi.org/10.1016/j.resplu.2020.100007>.

## References

- Benjamin EJ, Blaha MJ, Chiuve SE, et al. Heart disease and stroke statistics-2017 update: a report from the American heart association. *Circulation*. 2017;135:e146–e603.
- Laver S, Farrow C, Turner D, Nolan J. Mode of death after admission to an intensive care unit following cardiac arrest. *Intensive Care Med*. 2004;30:2126–2128.
- Moulaert VR, Verbunt JA, van Heugten CM, Wade DT. Cognitive impairments in survivors of out-of-hospital cardiac arrest: a systematic review. *Resuscitation*. 2009;80:297–305.
- Caro-Codon J, Rey JR, Lopez-de-Sa E, et al. Long-term neurological outcomes in out-of-hospital cardiac arrest patients treated with targeted-temperature management. *Resuscitation*. 2018;133:33–39.
- Lilja G, Nielsen N, Friberg H, et al. Cognitive function in survivors of out-of-hospital cardiac arrest after target temperature management at 33 degrees C versus 36 degrees C. *Circulation*. 2015;131:1340–1349.
- Leng Y, Liang MH, Ren M, Marinova Z, Leeds P, Chuang DM. Synergistic neuroprotective effects of lithium and valproic acid or other histone deacetylase inhibitors in neurons: roles of glycogen synthase kinase-3 inhibition. *J Neurosci*. 2008;28:2576–2588.
- Ren M, Leng Y, Jeong M, Leeds PR, Chuang DM. Valproic acid reduces brain damage induced by transient focal cerebral ischemia in rats: potential roles of histone deacetylase inhibition and heat shock protein induction. *J Neurochem*. 2004;89:1358–1367.
- Zhang C, Zhu J, Zhang J, et al. Neuroprotective and anti-apoptotic effects of valproic acid on adult rat cerebral cortex through ERK and Akt signaling pathway at acute phase of traumatic brain injury. *Brain Res*. 2014;1555:1–9.
- Gottlicher M, Minucci S, Zhu P, et al. Valproic acid defines a novel class of HDAC inhibitors inducing differentiation of transformed cells. *EMBO J*. 2001;20:6969–6978.
- Gurvich N, Tsygankova OM, Meinkoth JL, Klein PS. Histone deacetylase is a target of valproic acid-mediated cellular differentiation. *Canc Res*. 2004;64:1079–1086.
- Marinova Z, Ren M, Wendland JR, et al. Valproic acid induces functional heat-shock protein 70 via Class I histone deacetylase inhibition in cortical neurons: a potential role of Sp1 acetylation. *J Neurochem*. 2009;111:976–987.
- Jin G, Liu B, You Z, et al. Development of a novel neuroprotective strategy: combined treatment with hypothermia and valproic acid improves survival in hypoxic hippocampal cells. *Surgery*. 2014;156:221–228.
- Alam HB, Shuja F, Butt MU, et al. Surviving blood loss without blood transfusion in a swine poly-trauma model. *Surgery*. 2009;146:325–333.
- Li Y, Yuan Z, Liu B, et al. Prevention of hypoxia-induced neuronal apoptosis through histone deacetylase inhibition. *J Trauma*. 2008;64:863–870. discussion 70-1.
- Li Y, Liu B, Sailhamer EA, et al. Cell protective mechanism of valproic acid in lethal hemorrhagic shock. *Surgery*. 2008;144:217–224.
- Lee JH, Kim K, Jo YH, Lee MJ, Hwang JE, Kim MA. Effect of valproic acid combined with therapeutic hypothermia on neurologic outcome in asphyxial cardiac arrest model of rats. *Am J Emerg Med*. 2015;33:1773–1779.
- Oh JS, Tulasi J, Xiaodan R, Stacey WC, Neumar RW. Valproic acid combined with postcardiac arrest hypothermic-targeted temperature management prevents delayed seizures and improves survival in a rat cardiac arrest model. *Crit Care Med*. 2017.
- Lee JH, Kim K, Jo YH, et al. Effect of valproic acid on survival and neurologic outcomes in an asphyxial cardiac arrest model of rats. *Resuscitation*. 2013;84:1443–1449.
- Halaweish I, Bambakidis T, Chang Z, et al. Addition of low-dose valproic acid to saline resuscitation provides neuroprotection and improves long-term outcomes in a large animal model of combined traumatic brain injury and hemorrhagic shock. *J Trauma Acute Care Surg*. 2015;79:911–919. discussion 9.
- Biesterfeld BE, Williams AM, Pai MP, et al. Dose optimization of valproic acid in a lethal model of traumatic brain injury, hemorrhage and polytrauma in swine. *J Trauma Acute Care Surg*. 2019.
- Georgoff PE, Nikolian VC, Bonham T, et al. Safety and tolerability of intravenous valproic acid in healthy subjects: a phase I dose-escalation trial. *Clin Pharmacokinet*. 2017.
- Council NR. *Guide for the Care and Use of Laboratory Animals*. eighth ed. Washington, DC: The National Academies Press; 2011.
- Nikolian VC, Georgoff PE, Pai MP, et al. Valproic acid decreases brain lesion size and improves neurologic recovery in swine subjected to traumatic brain injury, hemorrhagic shock, and polytrauma. *J Trauma Acute Care Surg*. 2017.
- Fuss IJ, Kanof ME, Smith PD, Zola H. Isolation of whole mononuclear cells from peripheral blood and cord blood. *Curr Protoc Im*. 2009 (Chapter 7):Unit7 1.
- Neely MN, van Guilder MG, Yamada WM, Schumitzky A, Jelliffe RW. Accurate detection of outliers and subpopulations with Pmetrics, a nonparametric and parametric pharmacometric modeling and simulation package for R. *Ther Drug Monit*. 2012;34:467–476.
- Burns JW, Baer LA, Darlington DN, Dubick MA, Wade CE. Screening of potential small volume resuscitation products using a severe hemorrhage sedated swine model. *Int J Burns Trauma*. 2012;2:59–67.
- Allshire RC, Madhani HD. Ten principles of heterochromatin formation and function. *Nat Rev Mol Cell Biol*. 2018;19:229–244.
- Higgins GA, Georgoff P, Nikolian V, et al. Network reconstruction reveals that valproic acid activates neurogenic transcriptional programs in adult brain following traumatic injury. *Pharm Res (N Y)*. 2017;34:1658–1672.
- Marchion DC, Bicaku E, Daud AI, Sullivan DM, Munster PN. Valproic acid alters chromatin structure by regulation of chromatin modulation proteins. *Canc Res*. 2005;65:3815–3822.
- Felisbino MB, Gatti MS, Mello ML. Changes in chromatin structure in NIH 3T3 cells induced by valproic acid and trichostatin A. *J Cell Biochem*. 2014;115:1937–1947.
- Ungrecht R, Kutay U. Mechanisms and functions of nuclear envelope remodelling. *Nat Rev Mol Cell Biol*. 2017;18:229–245.
- Stephens AD, Liu PZ, Banigan EJ, et al. Chromatin histone modifications and rigidity affect nuclear morphology independent of lamins. *Mol Biol Cell*. 2018;29:220–233.
- Paulsen J, Liyakat Ali TM, Nekrasov M, et al. Long-range interactions between topologically associating domains shape the four-dimensional genome during differentiation. *Nat Genet*. 2019;51:835–843.
- Okubo T, Hayashi D, Yaguchi T, et al. Differentiation of rat adipose tissue-derived stem cells into neuron-like cells by valproic acid, a histone deacetylase inhibitor. *Exp Anim*. 2016;65:45–51.
- Vukicevic V, Qin N, Balyura M, et al. Valproic acid enhances neuronal differentiation of sympathoadrenal progenitor cells. *Mol Psychiatr*. 2015;20:941–950.
- Farzanehpour P, Horne MK, Aumann TD. Can valproic acid regulate neurogenesis in Nestin+ cells in the adult midbrain? *Neurochem Res*. 2017;42:2127–2134.
- Watanabe Y, Nakajima K, Ito Y, et al. Twenty-eight-day repeated oral doses of sodium valproic acid increases neural stem cells and suppresses differentiation of granule cell lineages in adult hippocampal neurogenesis of postpubertal rats. *Toxicol Lett*. 2019;312:195–203.

38. Higgins GA, Williams AM, Ade AS, Alam HB, Athey BD. Druggable transcriptional networks in the human neurogenic epigenome. *Pharmacol Rev.* 2019;71:520–538.
39. Munster P, Marchion D, Bicaku E, et al. Clinical and biological effects of valproic acid as a histone deacetylase inhibitor on tumor and surrogate tissues: phase I/II trial of valproic acid and epirubicin/FEC. *Clin Canc Res.* 2009;15:2488–2496.
40. Munster P, Marchion D, Bicaku E, et al. Phase I trial of histone deacetylase inhibition by valproic acid followed by the topoisomerase II inhibitor epirubicin in advanced solid tumors: a clinical and translational study. *J Clin Oncol.* 2007;25:1979–1985.